Available online at http://ajol.info/index.php/ijbcs

Int. J. Biol. Chem. Sci. 8(6): 2750-2772, December 2014

ISSN 1997-342X (Online), ISSN 1991-8631 (Print)

International Journal of Biological and Chemical Sciences

Original Paper

http://indexmedicus.afro.who.int

Formation of carbonyl compounds in lean premixed atmospheric-pressure Ethylene/O_2/N_2 flames

A. SEYDI [1,*], J. BIET[2], J. L. DELFAU[2] et C. VOVELLE[2]

[1]*Département de Chimie, Faculté des Sciences et Techniques Université, C. A. Diop, Dakar, Sénégal.*
[1]*LCSR-CNRS 1C, Avenue de la Recherche Scientifique, 45071 Orléans, France.*
[*]*Corresponding author; E-mail: aseydi@ucad.sn*

ABSTRACT

Motivated by a better understanding of lean-fuel combustion, the present study has determined experimentally the chemical structure of four lean ethylene-oxygen-nitrogen flames stabilized on the flat-flame burner at atmospheric pressure (φ = 0.47, 0.508, 0.693 and 0.81). Species mole fraction profiles were also computed by the Premix code (Chemkin II version) and three detailed reaction mechanisms .A very good agreement was observed between the main flame properties: reactants consumption, final products (CO_2, H_2O), main intermediates, and other hydrocarbons in small concentrations, and the modeling. A special care was brought to the examination of the relative importance of carbonyl compounds formation and consumption, mainly (CH_2O and CH_3CHO). Pathway analyses were performed to identify the formation from the direct consumption of ethylene through the C_2H_3 and CH_2HCO. Sensitivity analyses were also performed in order to delineate the most sensitive reaction on the formation and consumption of these two carbonyl compounds.
© 2014 International Formulae Group. All rights reserved.

Keywords: Flame structure, lean flames, ethylene, carbonyl compounds, combustion, mechanisms.

INTRODUCTION

Recent years have seen a gaining interest in lean combustion because it offers the potential of enhanced fuel economy and reduced pollutants formation (CO, soot, and NO_x) and especially the reduction of CO_2 emissions. This last species will be crucial in efforts to mitigate global warming due to green house effects. However, lean flames are subjected to two issues: instabilities that can eventually lead to extinction and the formation of new pollutants (oxygenated products of hydrocarbons, such as carbonyl compounds, and in particular aldehydes).

Oxygenated compounds are in important intermediate product in hydrocarbons oxidation and alcohol (Warnatz et al., 1984). Their emissions are harmful to the environment as well as to human health and they should be reduced. In the last decade, formaldehyde and acetaldehyde have been studied in several experimental setups for various temperature and pressure conditions: for CH_2O, in static reactors (Hay and Hessam, 1971), flow reactors (Vardanyan et al., 1971 and 1974; Hochgreb et al., 1990; Glarborg et al., 2003), shock tubes (Drummond, 1971; Dean et al., 1979, 1980; Hidaka et al., 1993a, 1993b; Eitener et al., 1998; Friedrichs et al.,

© 2014 International Formulae Group. All rights reserved.
DOI : http://dx.doi.org/10.4314/ijbcs.v8i6.34

2004) and flames (Oldenhove et al., 1986; Kaiser et al., 1991; Corr et al., 1992; Dagaud et al., 1994; Curran et al., 1998; Zervas et al., 1999, 2001, 2002, 2005; Dias et al., 2012); and for CH_3CHO, in static reactors (Kaiser et al., 1986), flow reactors (Colket et al., 1975, 1977), shock tubes (Dagaut et al., 1995; Won et al., 2000; Yasunaga et al., 2007) and flames (Leplat and Vandooren, 2010). All these past studies have allowed the determination of the consumption pathways of such carbonyl compounds.

All these past studies have allowed the determination of the consumption pathways of such carbonyl compounds. The study of the oxygenated pollutants, in particular, the carbonyl compounds formation in the simple flames is a step for understanding of their formation and emission in exhaust gas or industrial burners.

The objective of the present work is to identify the pathways of formation and consumption of these compounds in the combustion of a simple fuel, ethylene (C_2H_4). As a key intermediate in the oxidation of higher alkanes, ethylene plays an important role in the combustion mechanism of most practical fuels as well as in atmospheric chemistry. In rich conditions, ethylene is a precursor of aromatics and soot particles through the formation of acetylene (C_2H_2). Several researchers have carried out studies to improve the knowledge of ethylene oxidation. Recent measurements of the laminar flame velocity of ethylene-air mixtures have been reported (Jomaas et al., 2005). Tubular and jet stirred reactors have been used to derive analytical data at intermediate temperatures (Westbrook et al., 1982, 1988; Dagaut et al., 1988; Marivov et al., 1995). Ignition delays measured in shock tubes have been compiled recently by Varatharjan and Williams (2002).

The chemical structure of ethylene flames has been studied at low pressure by using molecular beam-mass spectrometer technique (Peeters et al., 1973; Law et al., 2005; Musik et al., 2000) and atmospheric pressure (Harris et al., 1986; Cool et al., 1988). The latter aimed at identifying aromatics and soot precursors and concerned essentially rich flames.

Detailed combustion mechanisms have been developed to reproduce the available experimental data on ethylene oxidation. They have been progressively improved by a better description of the various ethylene attack reactions by H, O and OH (Dagaut et al., 1988; Wilk et al., 1990; Marinov et al., 1995; Varatharjan et al., 2002). Specific studies on the kinetics of $C_2H_3 + O_2$ reactions (Westbrook et al., 1982; Bozzelli., 1993) have been also beneficial (Hidaka et al., 1999; Lindstedt et al., 2000).

With the development of premixed lean combustion to reduce soot and NO_X production, there is a need for data obtained in lean atmospheric flames. Indeed, few data of the ethylene oxidation are up to now available. Bhargava and Westmoreland (1998) studied the laminar flat $C_2H_4/O_2/Ar$ flame at the equivalence ratio of 0.75, at low pressure (40 mbar) to understand the ethylene oxidation. Later, Law et al. (2005) analysed a fuel-lean ethylene flat flame ($C_2H_4/O_2/Ar$, φ = 0.70, 40 mbar) enriched with allene (C_3H_4) to observe the influence of such hydrocarbons on the soot precursors formation. They did not focus their work on the ethylene oxidation but rather on the hydrocarbons formation due to the presence of C_3H_4. These two experimental works have been performed with argon as thinner but not nitrogen, and they worked at low pressure. Delfau et al. (2007) studied the laminar flat flame $C_2H_4/O_2/N_2$ at the equivalence ratios of 0.5 and 0.7, at atmospheric pressure, to understand the ethylene oxidation in lean conditions. Their objective was to check the ability of four detailed reaction mechanisms (Konnov, UCSD, UDEL and Dagaut) to correctly predict the temperature and species mole fraction profiles. Lopez et al. (2009) recently studied ethylene oxidation, through the analysis of $C_2H_4/O_2/N_2$ in a flow reactor, at high pressure (60 bar), for equivalence ratios ranging from 0.05 to 5. The objective was to develop and validate a kinetic model at high pressure instead of low pressure.

None of these previous works focused on the formation of oxygenated species for lean ethylene mixtures. In this work, the structures of four ethylene-oxygen-nitrogen flames with equivalence ratios of 0.47, 0.508, 0.693 and 0.81, diluted by nitrogen, were studied experimentally at atmospheric pressure, to observe the formation of the carbonyl compounds with nitrogen presence.

A special care was brought to the examination of the relative importance of various carbonyl compounds formation pathways, and the sensitivity analyses in order to delineate the most sensitive reaction on the formation and consumption of these two carbonyl compounds.

MATERIALS AND METHODS

The five ethylene-oxygen-nitrogen flames were stabilized on a flat-flame burner at atmospheric pressure. The upper part of the burner was made of a brass disk with small holes (1.0 mm diameter) drilled on a 4.0-cm-diametr circular area. Details have been more completely described elsewhere (Biet et al., 2005).

Table1 lists the initial conditions for the five flames studied, in term of parameters needed for simulations with the Premix code. The N_2/O_2 ratios were adjusted in order to improve the stability of leanest flames or to maintain a minimum distance between the flame front and burner surface for the richest ones.

Gas samples were taken along the symmetry axis of the flame by a quartz microprobe, mounted on a micrometer stage for vertical adjustment of the probe position relative to the burner surface. The probe was constructed from a 0.5-cm-diameter quartz tube drawn to a cone at the end. A hole (0.1 mm diameter) was drilled at the tip of this cone.

Gaseous samples were withdrawn from the flame through the probe and either directly injected into a gas chromatograph or stored in Pyrex sample flasks at a pressure limited to about 4 kPa to quench the chemical reactions within the hot tip of the probe.

Gaseous samples withdrawn from flame were analyzed either by gas chromatograph (GC) or by Fourier transform infrared spectroscopy (FTIR). For GC analyses, the gaseous samples where stored in Pyrex flasks at low pressure (2.0 kPa maximum) and compressed by a mechanical piston up to 53 kPa (Vovelle et al., 1971) prior injection into the chromatograph. This compression greatly enhances the detection limit which was estimated to be about 1 ppm. Helium was used as carrier gas for all species analyses, except H_2 which was measured with nitrogen to enhance the detector sensitivity.

Gaseous samples were collected directly in the FTIR cell up to 3.3 kPa. Species analyzed by GC were CH_4, C_2H_4, C_2H_2, C_2H_6, C_3H_6, C_3H_8, CO, CO_2, CH_3CHO, H_2, O_2, and N_2, CH_2O, H_2O, CO, and CO_2 were measured by FTIR.

Species calibration was performed by using a gaseous mixture of known composition. The accuracy was estimated to be ±5% for permanent gases and C_1 and C_2 hydrocarbons, ±10% for C_3H_6 and ±20% for CH_2O and CH_3CHO.

FTIR analyses were performed with the cell filled by the sampled gas up to 3.33 kPA. The selected spectral windows were 2118.3-2128.8 cm^{-1} for CO, 2379.3-2381.2 cm^{-1} for CO_2, 1716.6-1719.2 cm^{-1} for H_2O, and 1744.1-1746.7 cm^{-1} for CH_2O. For the latter, the signal had to be corrected for a contribution from H_2O.

Temperature profiles were measured by using a Pt/Pt-10%Rh thermocouple (Biet et al., 2003), made of 50 µm-diameter wires tightened parallel to the burner surface and coated with a BeO-Y_2O_3 deposit to reduce catalytic effects (Kent, 1970). Radiation losses were corrected using the classical electrical compensation technique (Bonne et al., 1960). The temperature profiles measured in the five flames with this new thermocouple have been plotted on Figure1. Based on measurement reproducibility the accuracy was estimated to 5%. Changes in the N_2/O_2 ratio, aimed at improving the flames stability, limit the variation of the maximum temperature to less

than 200 K when the equivalence ratio was decreased from 0.812 to 0.471.

Modelling

The lean flames structures were computed by using the Chemkin II (Kee et al., 1985) and Premix (Kee et al., 1980) code. Three detailed combustion mechanisms currently available on Web sites have been used to compute the species mole fraction profiles.

UDEL (Qin et al., 2000) mechanism is based upon addition of reactions for C_3 to C_6 species to the GRI-MECH mechanism (Smith et al., 1999). It includes 70 species and 455 reversible reactions.

The mechanism developed by (Konnov, 2000) is more detailed. In its original version, it contains 127 species: $C_XH_YO_Z$ from C_0 to C_6 and nitrogenous intermediates. These species are involved in 1158 reversible reactions and 49 nonreversible reactions. In this work, the N-species subsystem was removed so that the number of species was reduced to 93 and the number of reactions to 730 reversible and 47 no reversible.

The third mechanism has been developed by the Combustion Division of the Center for Energy Research at the University of California, San Diego (UCSD) with the objective to describe phenomena relevant to flame conditions with the number of reactions and species kept to minimum. The 2002 version (20021001) has been used in this work. It contains 39 species (up to C_3) involved in 179 reactions (167 reversible and 6 reactions with kinetic parameters given for the forward and reverse reactions).

Thermodynamic and transport data have been taken without any change from the respective Web sites.

Flame simulations were performed with the "BURN" option and experimental temperature profile introduced as input data. They were also conducted with the "FREE" option and use of the energy equation to derive the temperature profile. The latter procedure led to maximum temperatures only slightly higher than the measured ones, showing that due to care taken to stabilize each flame with an overall flow rate close to the maximum value compatible with flame stability, the five flames were almost adiabatic.

RESULTS

The experimental profiles were shifted to take into account the results of specific measurements performed with sampling probe and the thermocouple simultaneously present in the flame. These measurements showed that the probe did not influence the thermocouple signal when it was not connected to the vacuum pump. As soon as the pressure in the probe was reduced, to reproduce the sampling conditions, a marked reduction in the thermocouple signal was observed. An increase in the distance separating the probe and the thermocouple resulted in a progressive increase in the thermocouple signal up to the "unperturbed" value, measured with the probe located very far from the thermocouple. This maximum "perturbation distance" decreased when the pressure maintained in the probe was increased. It was also smaller at low temperature upstream the flame front. A shift position (z') was derived from the position of the sampling probe (z) from the expression:

$$z' = z\text{-}d \times \frac{T(z) - T_0}{T_{max} - T_0} \quad (1)$$

with T_0: temperature at the burner surface, T_{max}: maximum flame temperature and d: maximum shift distance. The latter increased when sampling pressure decreased and following values were used: 0.02 cm (GC_1), 0.05 cm (GC_2) and 0.03 cm (FTIR).

Flame temperature profiles

The experimental temperature profile constitutes an essential parameter for interpretation of laminar flame data. In both flames, the temperature gradient and burned gas temperature are very well reproduced by Konnov, UCSD mechanisms as shown in Figure 1, here only the leanest flame is represented. With UDEL mechanism, the

slope is smaller and the profile is shifted away from the burner surface. The very good agreement observed for the maximum temperature shows that experimental heat losses were reduced to a minimum and the flames were stabilized in adiabatic conditions. Final flame temperatures are 1736 K, 1685 K, 1901 K, 1765 K and 1760 K for the equivalence ratios of 0.47, 0.508, 0.70 and 0.81, respectively.

Reactants, main products and intermediates

Figures 2, 3 and 4 compare the computed and experimental mole fraction profiles for the reactants, main products and intermediates: CO_2, H_2O, CO, H_2. The down-stream shift noticed with UDEL mechanism for the temperature leads to a similar shift in the species mole fraction profiles. With Konnov, UCSD, and UDEL mechanisms the computed profiles are almost identical and perfectly reproduce the experimental evolutions. The three mechanisms predict post-flame concentrations in very good agreement with the experiments. Such a good agreement must be expected since in lean flames, CO_2 and H_2O are the only final products corresponding to the complete conversion of carbon and hydrogen.

In both flames, slight differences are observed in modelling of CO and H_2, as shown in Figure 5 and 8. The three mechanisms give very close profiles, in very good agreement with experimental data for H_2. Konnov's mechanism predicts very well the H_2 maximum concentration. Konnov and UCSD slightly overpredict CO, and UDEL mechanism predicts well the CO maximum concentration.

Hydrocarbons

Other intermediate species include hydrocarbons (Figures 9-12): propane, propene, ethane and acetylene, with experimental maximum concentration of 1.0×10^{-4}, 1.3×10^{-4}, 2.0×10^{-4} , 3.0×10^{-4} for ethane and $2.1.0\times10^{-4}$, 2.1×10^{-4}, 5.3×10^{-4} , $8.6.0\times10^{-4}$ for acetylene , for the equivalence ratios of 0.47, 0.508, 0.693 and 0.812 respectively (Figure 7), and methane, with experimental maximum concentration of $2.1.0\times10^{-4}$, $2.8.0\times10^{-4}$, $6.0.0\times10^{-4}$, 8.0×10^{-4}, for the equivalence ratios of 0.47, 0.508, 0.693 and 0.812 respectively (Figure 11). They are all consumed very fast so that their mole fraction profiles have a strong negative gradients after the maximum. A general agreement is observed between predicted and measured mole fraction profiles. These results are in accordance with those obtained by Delfau et al. (2007).

The three mechanisms give very similar profiles for all hydrocarbons. A more detailed examination shows that the predicted maximum mole fraction is very close to the experimental value for ethane and acetylene and slightly overestimated by the models for propane, propene, and methane. UDEL mechanism underpredicts the mole fraction profiles of all hydrocarbons measured.

Differences are observed for propane and propene, with UCSD mechanism predicting higher maximum value in propene than in propane. For ethane and acetylene, UCSD mechanism predicts very well the maximum mole fraction profiles.

Carbonyl compounds

Since they are potential pollutants of lean combustion, a special attention was brought to the analysis of these oxygenated species. Neither methanol nor acrolein could be detected, even in the leanest flame. These species should be analysed on the first gas chromatograph with a detection limit estimated to 100 ppm, so that it can be concluded that the maximum mole fraction is smaller than this value for both species. In the leanest flame, maximum mole fractions computed by the models were 1.09×10^{-4} (Konnov), 2.56×10^{-5} (UDEL), and 1.43×10^{-5} (UCSD) for methanol. Acrolein is involved only in the UDEL mechanism and its computed maximum mole fraction is 3.55×10^{-7}. Formaldehyde and acetaldehyde were present in the four flames studied. For the former, the maximum mole fraction is underpredicted by a factor of 2 by the UCSD mechanis, by a factor 3 by the UDEL mechanism whereas Konnov's predicts maximum values in very good agreement with the experiments (Figures 13 and 14).

Table 1: Initial conditions of five C_2H_4-O_2-N_2 flames (pressure: 101 kPa).

Mole fractions	Flame1	Flame 2	Flame 3	Flame 4	Flame 5
C_2H_4	0.0378	0.0364	0.0426	0.0390	0.0393
O_2	0.242	0.214	0.191	0.166	0.145
N_2	0.720	0.748	0.763	0.794	0.815
Mass flux ($gcm^{-2}s$-1)	0.0273	0.0218	0.0376	0.0252	0.0216
Equivalence ratio	0.471	0.508	0.693	0.703	0.813
N_2/O_2	2.9.75	3.495	3.998	4.783	5.624

Table 2: Effective equivalence ratio of ethylene/O_2/N_2 flames.

Exp/Model Φ	0,471	0,508	0,693	0,703	0,813
Exp	1,09	0,97	1,03	1,08	1,11
UDEL	1,01	1,01	1	1,01	1,03
Konnov	0,99	0,99	1	1,01	1,03
UCSD	1	1	1,01	1,01	1,01

Table 3: Effective equivalence ratio for lean flames.

Flame	Φ	Φeff	References
CH4/O2	0.17	1.02	(Fristrom et al., 1960)
CH4/O2	0.21	0.87	(Peeter et al., 1973)
CH4/O2/Ar	0.90	1.08	(Lazzara et al., 1973)
C2H4/O2/Ar	0.59	0.99	(Peeter et al., 1974)
C2H2/O2	0.12	1.29	(Vandooren et al., 1977)
CH2O/O2	0.26	0.83	(Oldenhove et al., 1983)
C3H8/O2/N2	0.80	0.99	(Bockhom et al., 1991)
C2H2/O2/Ar	0.88	1.20	(Volpini et al., 1992)
C3H6/O2/Ar	0.23	1.08	(Thomas et al., 1996)
C7H16/O2/N2	0.70	1.03	(El Balkali., 2003)
C8H18/O2/N2	0.70	1.03	(El Balkali., 2003)
C2H4/O2/Ar	0.75	1.11	(Bhargava et al., 1998)
C3H8/O2/N2	0.48	1.11	(Biet et al., 2005)

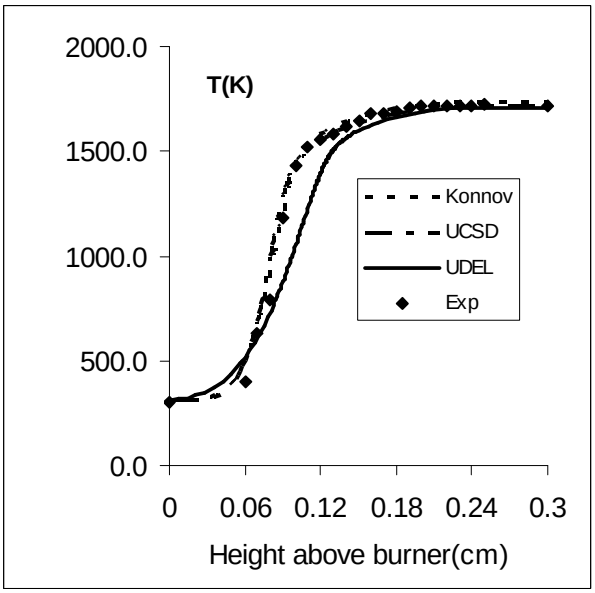

Figure 1: Computed (lines) and measured (symbols) temperature profile in ethylene/O_2/N_2 at the equivalence ratio of 0.47.

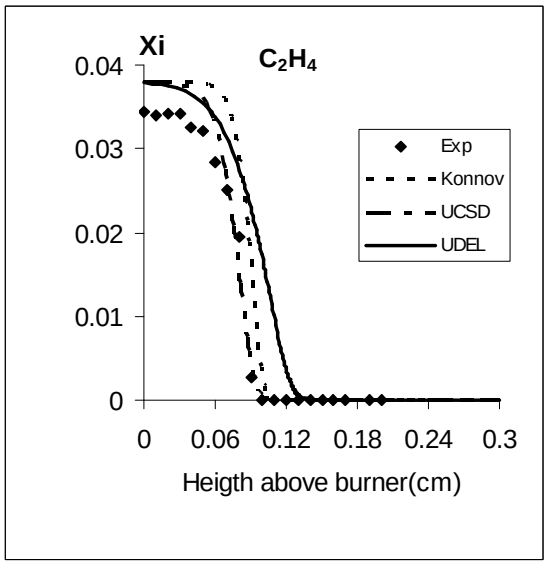

Figure 2: Computed (lines) and measured (symbols) mole fraction profiles (Xi) of C_2H_4 in the ethylene /O_2/N_2 flame at equivalence ration of 0.47.

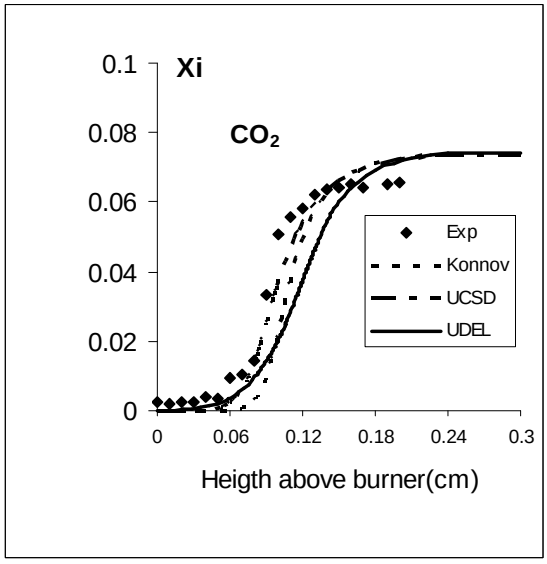

Figure 3: Computed (lines) and measured (symbols) mole fraction (Xi) profiles of CO_2 in the ethylene /O_2/N_2 flame at equivalence ration of 0.47.

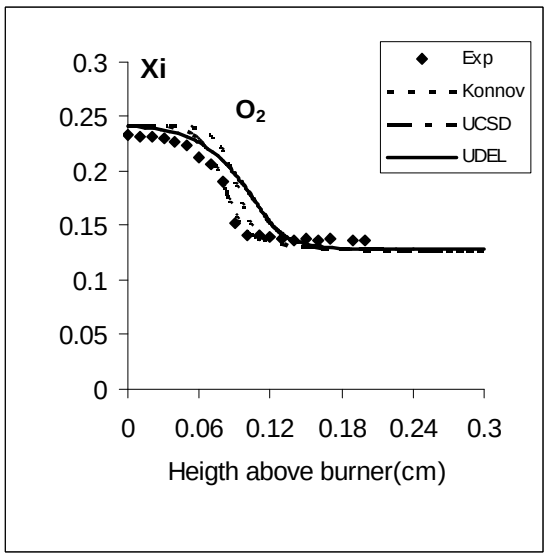

Figure 4: Computed (lines) and measured (symbols) mole fraction profiles (Xi) of O_2 in the ethylene /O_2/N_2 flame at equivalence ration of 0.47

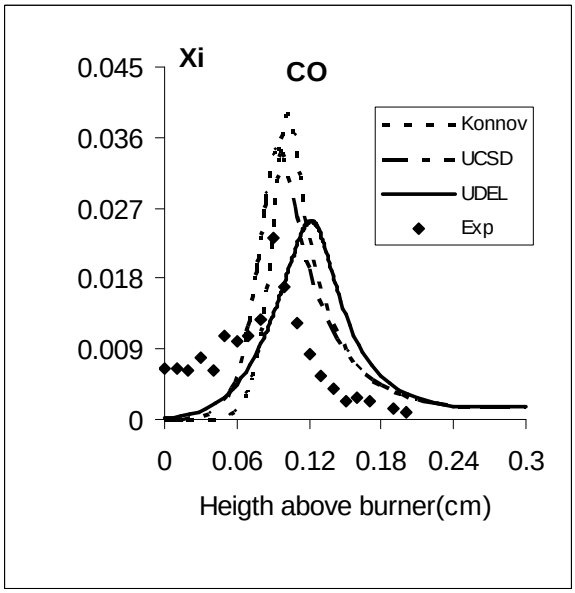

Figure 5: Computed (lines) and measured (symbols) mole fraction (Xi) profiles of CO in the ethylene /O_2/N_2 flame at equivalence ration of 0.47

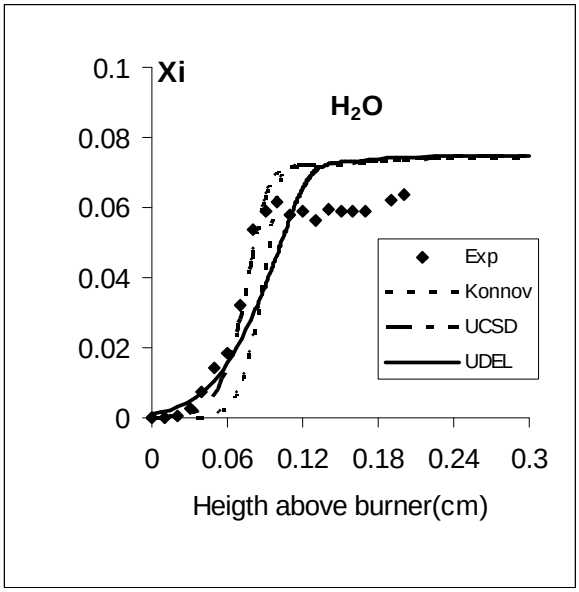

Figure 6: Computed (lines) and measured (symbols) mole fraction (Xi) profiles of H_2O in the ethylene /O_2/N_2 flame at equivalence ration of 0.47.

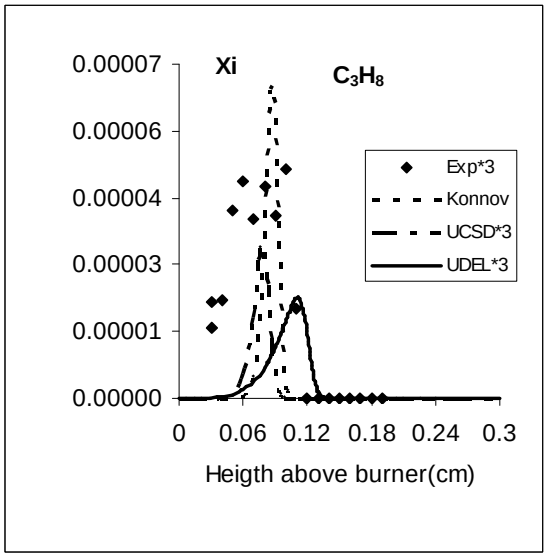

Figure 7: Computed (lines) and measured (symbols) mole fraction (Xi) profiles of C_3H_8 in the ethylene /O_2/N_2 flame at equivalence ration of 0.47.

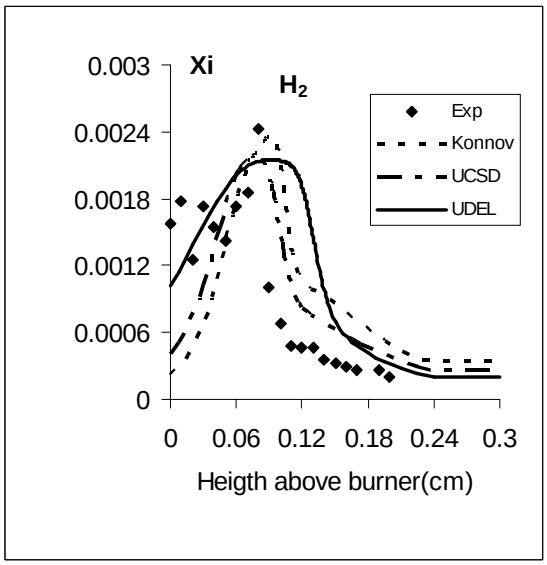

Figure 8: Computed (lines) and measured (symbols) mole fraction (Xi) profiles of H_2 in the ethylene /O_2/N_2 flame at equivalence ration of 0.47.

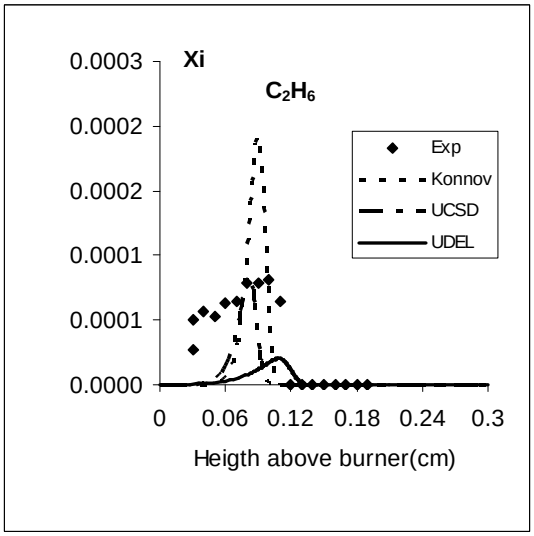

Figure 9: Computed (lines) and measured (symbols) mole fraction (Xi) profiles of C_2H_6 in the ethylene /O_2/N_2 flame at equivalence ration of 0.47.

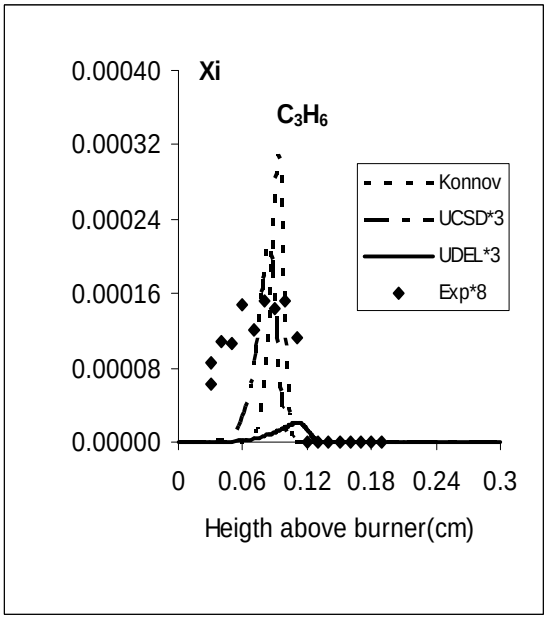

Figure 10: Computed (lines) and measured (symbols) mole fraction (Xi) profiles of C_3H_6 in the ethylene /O_2/N_2 flame at equivalence ration of 0.47.

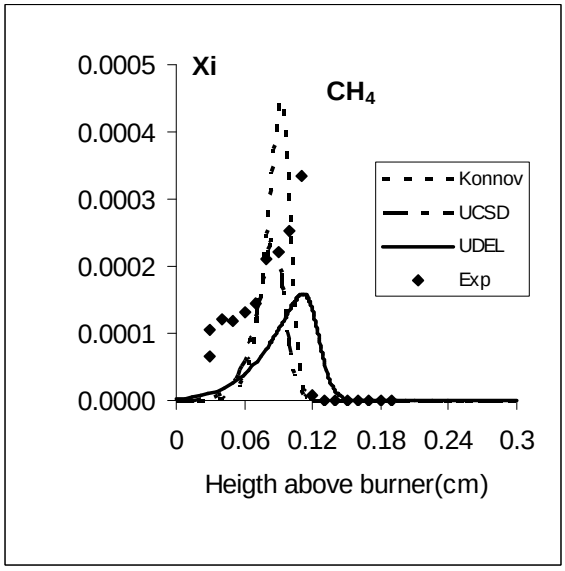

Figure 11: Computed (lines) and measured (symbols) mole fraction (Xi) profiles of CH_4 in the ethylene /O_2/N_2 flame at equivalence ration of 0.47.

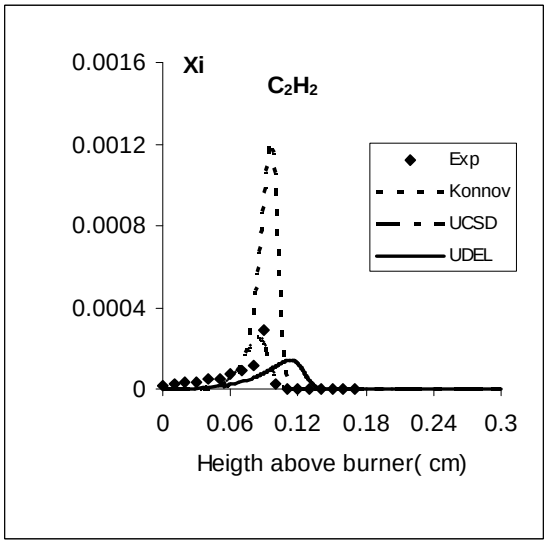

Figure 12: Computed (lines) and measured (symbols) mole fraction (Xi) profiles of C_2H_2 in the ethylene /O_2/N_2 flame at equivalence ration of 0.4.

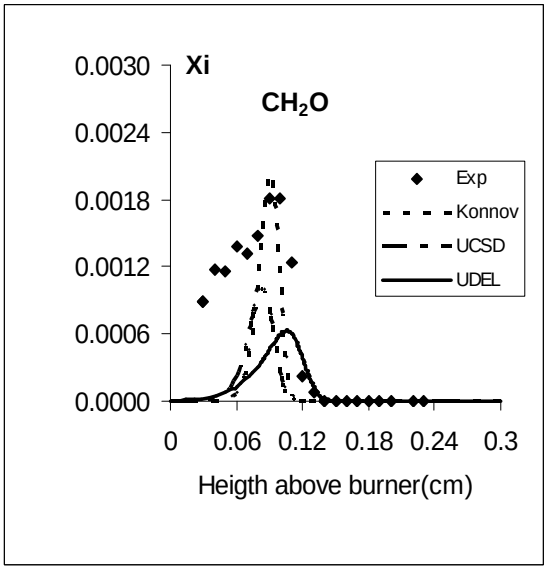

Figure 13: Computed (lines) and measured (symbols) mole fraction (Xi) profiles of CH_2O in the ethylene /O_2/N_2 flame at the equivalence ratio of 0.47.

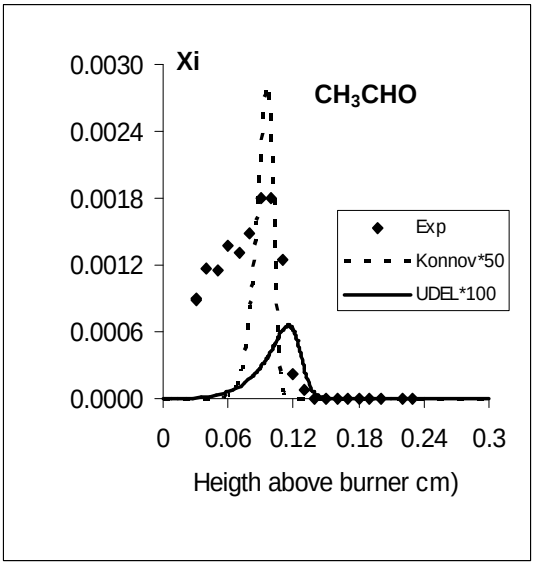

Figure 14: Computed (lines) and measured (symbols) mole fraction (Xi) profiles of CH_3CHO in the ethylene /O_2/N_2 flame at the equivalence ratio of 0.47.

DISCUSSION

C_2H_4 kinetics

Figure 15 compares the main ethylene consumption route in the leanest flame (φ = 0.47). Only small variations are in the others equivalence ratios and the main differences identified from these mechanisms are common to both flames. The sequence and relative importance of reactions in this flame were examined with reaction path analysis.

For clarity purpose, the consumption paths are split into three parts: (i) the first steps in the fuel consumption, (ii) and (iii) the consumption of the main intermediates formed in (i): the vinyl and the vinoxy radical, respectively.

According to these mechanisms, ethylene is mainly consumed by reactions $C_2H_4 + O \rightarrow CH_3 + HCO$ (R.1), largely dominant 63% in UDEL mechanism, and contributes only to 22% and 37% in Konnov and UCSD mechanisms, respectively. In the Konnov mechanism, OH addition to C_2H_4: $C_2H_4 + OH \rightarrow CH_3 + CH_2O$ (R.2)) also contributes and the sum of reactions (R.1) and (R.2) represents 35.7% of the fuel conversion.

The main intermediates in ethylene consumption are the vinyl and vinoxy radicals formed by the reactions: C_2H_4 + O, OH, H → C_2H_3 + OH, H_2O, H_2 (R.3) and reaction: $C_2H_4 + O \rightarrow CH_2HCO + H$ (R.4).

C_2H_3 kinetics

The main consumption of C_2H_3 is due to the reaction with oxygen molecule to produce the vinoxy radicals $C_2H_3 + O_2 \rightarrow CH_2HCO + O$ (R.5), and formaldehyde $C_2H_3 + O_2 \rightarrow CH_2O + HCO$ (R.6). The C_2H_3 is also directly responsible for the formation of hydrocarbons such as C_2H_2:$C_2H_3 + O_2 \rightarrow C_2H_2 + HO_2$ (R.7), with a contribution of 11.6% (Konnov), 4.1% (UCSD) and 3.3% (UDEL), respectively, and C_3H_6: $C_2H_3 + CH_3 + M \rightarrow C_3H_6 + M$ (R.8), with the same negligible contributions in the three mechanisms, for the 0.47 ethylene flame. The acetylene is then destroyed by O-atom reaction, and produces the ketenyl radical, by the reaction: $C_2H_2 + O \rightarrow HCCO + H$ (R.9). This reaction (R.9) is the main pathway of formation for HCCO, with a contribution of 16% (Konnov), 2.35% (UCSD) and 2.96% (UDEL), respectively. The consumption of C_3H_6 allows the formation of C_3H_5 radical in the flames by the reaction: $C_3H_6 + OH \rightarrow C_3H_5 + H_2O$ (R.10).

The C_3H_5 radical consumption forms the propene through the reaction: $C_3H_5 + H + M \rightarrow C_3H_6 + M$ (R.11), and, also the allene (a-C_3H_4) through the reactions: $C_3H_5 + H \rightarrow$ a-$C_3H_4 + H_2$ (R.12), and reaction: $C_3H_5 + OH \rightarrow$ a-$C_3H_4 + H_2O$ (R.13).

Figure 19 clearly shows that different situation is observed when the consumption of vinoxy radical is considered. Indeed, the formation of ketene is common to the three mechanisms. It is the unique vinoxy radical consumption path in the UCSD mechanism (45.5%), it occurs dominantly in the UDEL mechanism (13.3%) whereas it is only a secondary path in Konnov mechanism (10.2%). In Konnov mechanism, CH_3CO is the main intermediate (16.1%).

According to the three mechanisms, the methane is produced from the methyl radical by the reaction: $CH_3 + H + (M) \rightarrow CH_4 + M$ (R.14), with a contribution of 2.36% (Konnov), 3.73% (UCSD) and 4.40% (UDEL) for the ethylene 0.47 flame, and its main destruction leads to methyl radical formation by the reaction: $CH_4 + OH \rightarrow CH_3 + H_2O$ (R.15).

By recombination of CH_3, the ethane (C_2H_6) is produced in the flames with a contribution of 12.2% (Konnov), 5% (UCSD) and 3.15% (UDEL), respectively, and its main consumption leads to the production of C_2H_5 by the reaction: $C_2H_6 + OH \rightarrow C_2H_5 + H_2O$ (R.16).

One of the consumption pathways of the C_2H_5 radicals allows the formation of propane (C_3H_8), by reaction with methyl radical: $C_2H_5 + CH_3 \rightarrow C_3H_8$ (R.17), with small contribution in the three mechanisms, for the ethylene of 0.47.

In the ethylene flame, the formation of acetylene (C_2H_2) comes directly from the consumption of vinyl radical (C_2H_3), by the

reactions: $C_2H_3 + O_2 \rightarrow C_2H_2 + HO_2$ (R.18), with a contribution of 11.6% (Konnov), 4.1% (UCSD) and 3.3% (UDEL), respectively.

Carbonyl compounds kinetics

According to these mechanisms, the main formation of CH_2O comes from the vinyl radical (C_2H_3) by the reaction (R.6), with a contribution of 7.0% (Konnov), 11.4% (UCSD) and 13.7% (UDEL) for the 0.47 flame, respectively. Also, its formation comes from directly to the ethylene consumption, with a contribution about 14% in Konnov mechanism. The main formaldehyde consumption produces the formyl radical (HCO) with the reaction: $CH_2O + O \rightarrow HCO + OH$ (R.19).

These two last reactions (R.6) and (R.19) are the most important reactions for the HCO formation with a major contribution for (R.7): 7.0% (Konnov) against 13.7% (UCSD), 11.4 (UDEL) for the equivalence ratio of 0.47, respectively. HCO goes rapidly to carbon monoxide (CO) and then to carbon dioxide (CO_2) by the reactions: $HCO + O_2 \rightarrow CO + HO_2$ (R.20), $CO + OH \rightarrow CO_2 + H$ (R.21).

The other carbonyl compound produced in these lean ethylene flames is the acetaldehyde (CH_3CHO). The main production of acetaldehyde comes also from the vinyl radical with the reaction $C_2H_3 + OH \rightarrow CH_3CHO$ (R.22), with a contribution of 2.3% (Konnov), this species is not included in UCSD mechanism, and negligible in (UDEL) mechanism for the ethylene 0.47 flame. Its consumption leads to the formation of acetyl radical (CH_3CO) by the reactions $CH_3CHO + OH \rightarrow CH_3CO + H_2O$ (R.23) and $CH_3CHO + H \rightarrow CH_3CO + H_2$ (R.24), with a contribution less than 1% (Konnov). These two reactions are negligible in UDEL mechanism. Then, by decomposition, the acetyl radical produces methyl radical and carbon monoxide: $CH_3CO + M \rightarrow CH_3 + CO + M$ (R.25), with 9.5% (Konnov), and negligible in (UCSD) and (UDEL) mechanisms.

A more careful examination shows that no differences are noticeable at maximum mole fraction of these two carbonyl compounds considering the experimental uncertainties estimated at 20% (Figures 13 and 14). With oxygen in excess, all hydrocarbons formed as intermediate species are oxidized by reactions with O_2, OH, O, and HO_2. The maximum concentration is around 1.8×10^{-3} for CH_2O and CH_3CHO. We can also observe that the final products CO_2 and HO_2. Have their concentrations controlled by the initial fuel content and these final mole fractions are similar in all the flames, around 7.0×10^{-2} (Figures 3 and 6).

These observations can be confirmed by calculating for each flame an "effective equivalence" ratio based on the proportion of oxygen consumed in the flame,

$$\Phi_{\text{eff}} = \frac{X_{C2H4i}}{(X_{O_2}i - X_{O_2f})} \times 3$$

Where X_{C2H4} and X_{O2} are the fuel and oxygen mole fractions and subscripts i and f denote the initial and final compositions, the coefficient 3 is the stoichiometric factor for C_2H_4.

Values obtained from experiments and from modelling with the three mechanisms are listed in Table 2.

All simulations lead to values very closed to 1.0. The higher values observed with the experimental results are related to the final oxygen concentrations which are systematically above the computed values.

It was interesting to use published results on the structure of lean flames to perform the same calculations. Flame structure studied covering a large domain of equivalence ratios and different fuels have been considered and their effective equivalence ratios are grouped in Table 3.

These experiments also produced values very closed to 1.0 for the effective equivalence ratio. The few discrepancies observed are due to uncertainties that affected the determination of the final O_2 mole fraction. At least, one of the sources of these uncertainties is a perturbation of the diffusion induced by the sampling probe. Uncertainty for this species was determined by

propagation-of-errors analysis to be 10%. The constant value calculated for the effective equivalence ratio leads to the conclusion that lean flames are stoichiometric flames diluted by a mixture composed of inert constituent, usually nitrogen, and oxygen in excess. Flames extinction at the lean stability limit would not correspond to a change in the combustion chemistry but rather to a marked decrease in temperature.

In this study, we have carried out sensitivity analyses in order to delineate the most sensitive reaction on the formation and consumption of these two carbonyl compounds. For this, the variation of the sensitivity coefficients is investigated with the equivalence ratio in terms of the sensitivity of mass fraction, in four ethylene flames (φ= 0.471; 0.693; 0.703; 0.813).

Sensitivities of mass fraction for formaldehyde

The sensitivity of mass fraction for the carbonyl species in all mechanisms, are presented in Figures 16 to 20 for lean ethylene flames. In the Konnov's mechanism, reactions: $CH_2O + OH \rightarrow HCO + H_2O$ (R.26) and reaction: $H + O_2 \rightarrow O + OH$ (R.27), are the most sensitive.

The sensitivity of reaction (R.26) varies slightly with the equivalence ration, whereas which of reaction (R.27) increases with the equivalence. Three other reactions: $CO + OH \rightarrow CO_2 + H$ (R.28), $CH_3 + HO_2 \rightarrow CH_3O + OH$ (R.29), and $CH_2O + H \rightarrow HCO + H_2$ (R.30), have also, high sensitivity coefficients. The sensitivity of reaction: $C_2H_4 + OH \rightarrow CH_2O + CH_3$ (R.2), varies slightly with the equivalence ratio.

As observed in Konno's mechanism, reactions (R.26) and (R.27) have the highest sensitivity coefficients in UCSD mechanism. The reactions $CH_3 + HO_2 \rightarrow CH_3O + OH$ (R.32), (R.3), (R.28) have also high sensitivity coefficients, but reaction (R.4) is the most sensitive reaction for the mass fraction of formaldehyde.

In UDEL mechanism, reaction (R.28) is the most sensitive .The reactions (R.30), and (R.29) keep the sensitivity coefficients high. One of the characteristics of this mechanism is the influence of the equivalence ratio on the sensitivity of reaction $H + O_2 \rightarrow O + OH$ (R.31). This sensitivity decreases when the equivalence ratio increases and increases in the leanest conditions, whereas reaction $H + HO_2 \rightarrow O_2 + H_2$ (R.32) is relatively sensitive in lean conditions.

Sensitivities of mass fraction for acetaldehyde

The analysis of sensitivity coefficients for acetaldehyde was performed using the Konnov and UDEL mechanisms. The sensitivity coefficients for these two mechanisms are presented in Figures 15 and 20 for the lean ethylene-air flames.

In Konnov's mechanism, reaction: $H + O_2 \rightarrow O + OH$ (R.33) is the most sensitive. Reactions: $CO + OH \rightarrow CO_2 + H$ (R.28), $CH_3CHO + OH \rightarrow CH_2HCO + H_2O$ (R.34), and $HCO + (M) \rightarrow CO + H + (M)$ (R.34), $H + O_2 + M \rightarrow HO_2 + M$ (R.35), also, have high sensitivity coefficients.

Some reactions are sensitive to a fuel, specifically, reaction: $C_2H_4 + OH \rightarrow C_2H_3 + H_2O$ (R.3).

As observed in Konnov mechanism, reaction: $H + O_2 \rightarrow O + OH$ (R.31), is one of the most sensitive reaction in UDEL mechanism, for the mass fraction of acetaldehyde whatever the equivalence ratio.

Reaction (R.28), also has an important sensitivity coefficient. Evenly, reaction: $C_2H_5 + O \rightarrow CH_3HCO + H$ (R.36), is particularly sensitive to acetaldehyde.

According to the results of the sensitivity coefficients of these carbonyl compounds, we can conclude that the chemistry of lean flames is not affected for the three mechanisms in the ethylene flames.

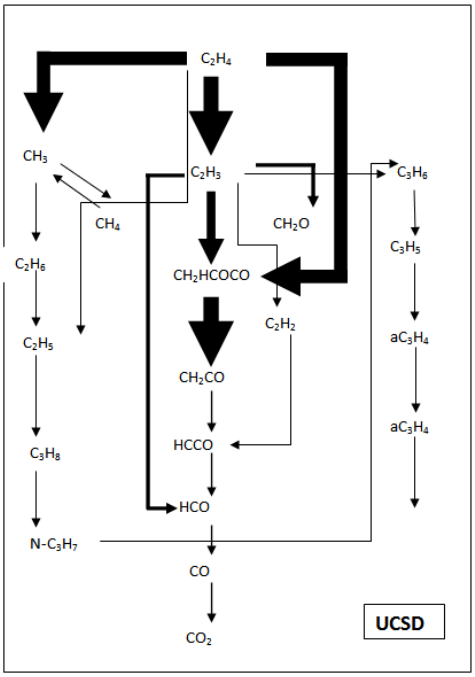

Figure 15: Pathways analyse in the leanest (φ = 0.47) ethylene flame.

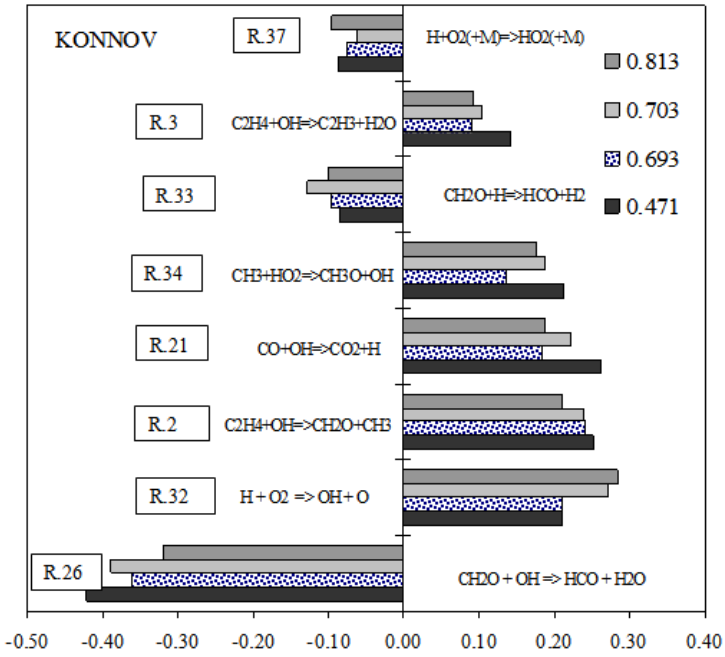

Figure 16: Sensitivity analysis for mass fraction of CH_2O in lean ethylene flames in Konnov mechanism.

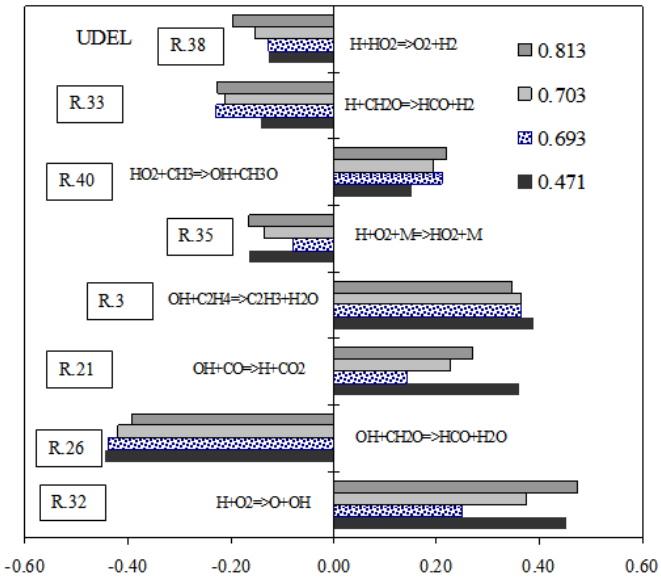

Figure 17: Sensitivity analysis for mass fraction of CH_2O in lean ethylene flames in UDEL mechanism.

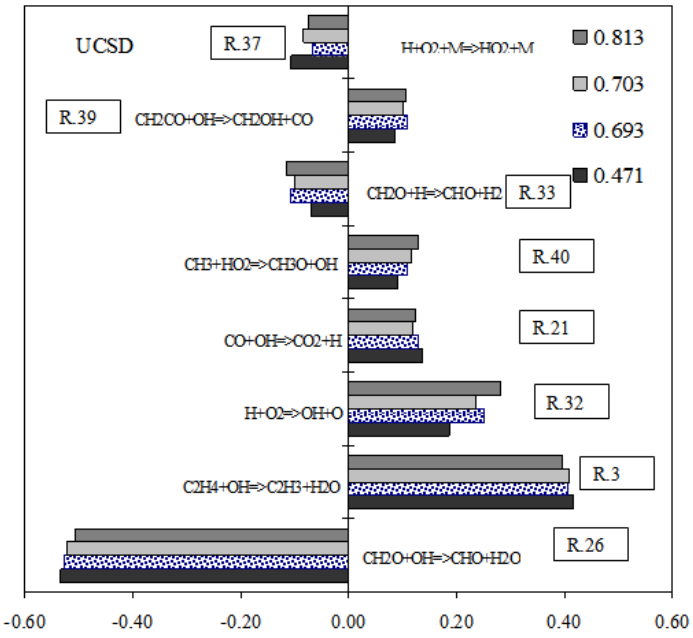

Figure 18: Sensitivity analysis for mass fraction of CH_2O in lean ethylene flames in UCSD mechanism.

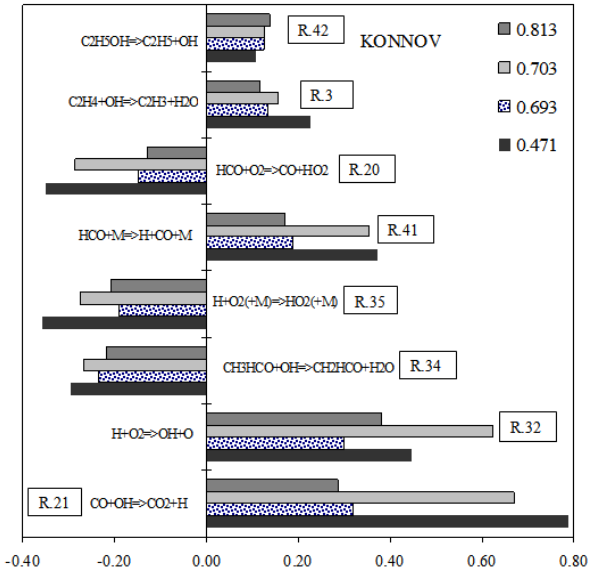

Figure 19: Sensitivity analysis for mass fraction of CH_3CHO in lean ethylene flames in Konnov mechanism.

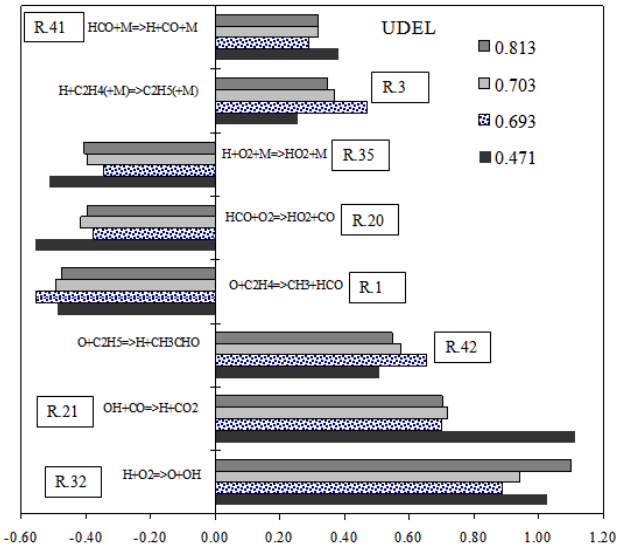

Figure 20: Sensitivity analysis for mass fraction of CH_3CHO in lean ethylene flames in UDEL mechanism.

Conclusion

The structures of premixed ethylene/oxygen/nitrogen flames at four equivalence ratios (0.47, 0.508, 0.693 and 0.81) have been studied by gas chromatography and by FTIR, at atmospheric pressure. Temperature measurements were made with a Pt/Pt-10%Rh thermocouple, and a good agreement was observed between experimental and model.

The very good agreement observed for the reactants consumption and the final products formation constitutes a minimum requisite since in very lean flames CO_2 and H_2O are the only final forms for C and H conversion, respectively. On the other hand, differences between mechanisms were observed when the prediction of the mole fraction profiles of the active intermediate species was considered. Pathways analyse helped in identifying the main causes of these differences. It was shown that the same reactions were involved in the three mechanisms to describe the consumption of ethylene, but with marked differences in their relative importance. C_2H_3 and CH_2HCO are the main radicals formed in the first step and their consumption increases the differences between the mechanisms either by use of different kinetics data for common reactions or by differences in the nature of consumption reactions.

The intermediate oxygenated species such as formaldehyde and acetaldehyde, are potential pollutants of lean flames, special attention was paid for their formation and consumption mechanisms. Sensitivities analyse allows to identify the reactions which influence the concentrations of these carbonyl compounds.

.

ACKNOWLEDGMENTS

Financial supports from the Region Centre (J.Biet grant) and from EGIDE (A.Seydi fellowship of the French Foreign Office) are greatly appreciated.

REFERENCES

Bhargava A, Westmorland PR. 1998. MBMS Analysis of a Fuel-Lean Etylene Flame. *Combust. Flame*, **115**: 456-467.

Biet J, Seydi A, Delfau JL, Vovelle C. 2003. Experimental and numerical study of the combustion chemistry of fuel-lean, laminar premixed flames stabilizided at atmospheric pressure. Proc. Eur. Combust. Meeting., ECM2003: 159.

Biet J, Delfau J-L, Seydi A, Vovelle C. 2005. Experimental and modeling study of lean premixed atmospheric pressure propane/O_2/N_2 flames. *Combust. Flame*, **142**: 197-209.

Bockhorn H, Chevalier CH, Warnatz J, Weyrauch V. 1991. Heat-Transfer in Fire and Combustion Systems, ASME.HDT, 166.

Bonne U, Grewer Th, Wagner HGg. 1960. Messungen in der Reaktionszone von Wasserstoff-Sauerstoff – und Methan – Sauerstoff-Flammen. *Z. Phys. Chem.*, **26**: 93.

Bozzelli J.W Dean AM. 1999. Hydrocarbon radical reactions with O_2: Comparison of allyl, formyl and vinyl to ethyl. *J. Phys. Chem.*, **97**: 4427-4441.

Corre C, Dryer FL, Pitz WJ, Bestbrook CK. 1992. Two stage n-butane flame: A comparative between experimental measurements and modelling results. *Proc. Combust. Inst.*, **24**: 843-850.

Curran HJ, Gaffuri P, Pitz WJ, Westbrook CK. 1998. A comprehensive modelling study of n-heptane oxidation. *Combustion and Flame*, **114**: 149-177.

Colket MB, Naegeli DW, Glassman J. 1975. High-temperature pyrolysis of acetaldehyde. *Int. J. Chem. Kinetic*., **7**: 223.

Cool TA, Bernstein JS, Song XM, Goodwin PM. 1989. Profiles of HCO and CH_3 in CH_4/O_2 and C_2H_4/O_2 flames by resonance ionization. *Proc. Combust. Inst.*, **22**: 1421-1432.

Dagaut P, Cathonet M, Bottner JC, Gaillard F. 1988. Kinetic modeling of ethylene oxidation. *Combust. Flame,* **71**: 295-312.

Dagaud P, Reuillon M, Cathonet M. 1994. High pressure oxidation of liquid fuels from low to high temperatures of n-heptane and isooctane. *Combust. Sci. Tech.,* **95**: 233-260.

Dagaut P, Reuillon M, Voisin D, Cathonnet M, McGuinness M, Simmie JM. 1995. Acetaldehyde oxidation in a JSR and ignition in shock waves: Experimental and comprehensive kinetic modelling. *Combust. Sci. Tech.,* **107**: 301.

Davis SG, Law CK, Wang H. 1999. Propene pyrolysis and oxidation kinetics in a flow reactor and laminar flames. *Combust. Flame,* **119**: 375-399.

Dean A, Craig B, Johnson R, Schultz M, Wang E. 1979. Shock tube studies of formaldehyde pyrolysis. *Proc. Combust. Inst.,* **17**: 577.

Dean A, Johnson R, Steiner D. 1980. Shock tube studies of formaldehyde oxidation. *Combust. Flame*, **37**: 41.

Delfau JL, Biet J, Idir M, Pillier L, Vovelle C. 2007. Experimental and numerical study of premixed lean ethylene flames. *Proc. Combust. Inst.,* **31**: 357-365.

Dias V, Duynslaegher C, Contino F, Vandooren J, and Jeanmart H. 2012. Experimental and modeling study of formaldehyde combustion in flames. *Combust. Flame,* **159**: 1814.

DiasV, Vandooren J, Jeanmart H. 2014(b). An experimental and modelling study of the addition of acetone to H_2/O_2/Ar flames at low pressure.L Proc.Combust.Inst., doi:10.1016/j.proci.201405.055.

Drummond L. 1971. Shock initiated Oxidation of Formaldehyde. *Combust. Sci. Tech.*, **3**: 47.

Eiteneer B, Yu C, Goldenberg M, Frenklach M. 1998. Determination of rate coefficients for reactions of formaldehyde pyrolysis and oxidation in the gas phase. *J. Phys. Chem. A.,* **102**: 5196.

Friedrichs G, Davidson D, Hanson R. 2004. Validation of a thermal decomposition mechanism of formaldehyde by detection of CH_2O and HCO behind shock waves. *Inter. J. Chem. Kinet.,* **36**: 157.

Fristrom RM, Grunfelder C, Favin S. 1960**.** Methane-oxygen flame structure**.** *J. Phys. Chem.*, **64**: 1386-1392**.**

Glarborg P, Alzueta M, Kjaergaard K, Dam-Johansen K. 2003. Oxidation of formaldehyde and its interaction with nitric oxide in a flow reactor. *Combust. Flame.*, **132**: 629.

Hay J, Hessam K. 1971. The oxidation of gaseous formaldehyde. *Combust. Flame,* **16**: 237.

Hidaka Y, Taniguchi T, Kamewasa M, Masaoka H, Inami K, Kawano H. 1993a. High temperature pyrolysis of formaldehyde in shock waves. *Inter. J. Chem. Kinetics*, **25**: 305.

Hidaka Y, Taniguchi T, Tanaka H, Kamewasa M, Inami K, Kawano H. 1993b. Shock-tube study of CH_2O pyrolysis and oxidation. *Combust. Flame,* **92**: 365.

Hidaka Y, Nishimori T, Sato K, Henmi Y, Okuda R, Inami K. 1999. Schock tube and modeling of ethylene pyrolysis and oxidation. *Combust. Flame,* **117**: 755-776.

Hochgreb S, Yetter R, Dryer F. 1990. The oxidation of CH_2O in the intermediate temperature range (943-955K). *Proc. Combust. Inst.*, **23**: 171.

Jomaas G, Zheng X.L, Zhu DL, Law CJ. 2005. Experimental determination of counterflow ignition temperatures and laminar speeds of C_2-C_3 hydrocarbon at atmospheric and elevated pressure. *Proc. Combust. Inst.,* **30**: 193-200.

Kaiser EM, Westbrook CK, Pitz WJ. 1986. Acetaldehyde oxidation in the negative temperature coefficient regime: Experimental and modelling results. *Int. J. Chem. Kinetics.,* **18**: 655.

Kaiser EW, Siegel WO, Henig YI, Anderson RW, Trinker FH. 1991. Effect of fuel structure on emissions from a spark-ignited engine. *Environ. Sci. Technol.,* **25**: 2005-2012.

Kee RJ, Rupley FM, Miller JA. 1989. ChemkinII: A Fortran Chemical Kinetics Package for analysis of Gas Phase Chemical Kinetics, Sandia Report SAND89-8009B.

Kee RJ, Grear JF, Smooke MD, Miller JA. 1985. A Fortran Program for modelling Steady Laminar One-Dimensional Premixed Flames, Sandia Technical Report SAND85-8240.

Kent JH. 1970. A noncatalytic coating for platinium-rhodium thermocouples. *Combust. Flame,* **14**(2): 279.

Konnov AA. 2000. A Detailed reaction mechanism for small hydrocarbons Combustion Release 0.5, available at: http://homepages.vub.ac.be/~akonnov/

Lazzara CP, Biordi JC, Papp JF. 1973. Concentration profiles for radical species in a methane-oxygen-argon flame. *Combust. Flame,* **21**(3): 371-382.

Law ME, Carrière T, Westmoreland PR. 2005. Allene addition to a fuel-lean ethylene flame. *Proc. Combust. Inst.,* **30**: 1353.

Leplat N, Vandooren J. 2010. Experimental investigation and numerical simulation of the structure of CH_3CHO/O_2/Ar flames at different equivalence ratios. *Combust. Sci. Tech,* **182**: 436.

Lindstedt RP, Skevis G. 2000. Molecular growth oxygenated species formation in laminar ethylene flames. *Proc. Combust. Inst.,* **28**: 1801-1807.

Lopez JG, Rasmussen CL, Alzueta MU, Gao Y, Marshall P, Glarborg P. 2009. Experimental and kinetic modeling study of C_2H_4 oxidation at high pressure. *Proc. Combust. Inst.,* **32**: 367.

Marinov NM, Malte PC. 1995. Ethylene oxidation in a well-stirred reactor. *Int. J. Chem. Kinetics,* **27**: 957-986.

Musik M, Vandooren J, Van Tiggelen PJ. 2000. Flame structure studies of several premixed ethylene-oxygen-argon flames at equivalence ratios from 1.00 to 2.00. *Comb. Sci. Tech* , **153**: 247-261.

Oldenhove de Guertechin L, Vandooren J, Van Tiggelen PJ. 1986. Kinetics in a lean formaldehyde flame. *Combust. Flame,* **64**: 127.

Peeters J, Mahnen G. 1973. Reaction mechanism and rate constant of elementary steps in CH_4/O_2 flames. *Proc. Combust. Inst,* **14**: 133-146.

Peeters J, Vinkier C, 1975. Production of chim-ions and formation of CH and CH_2 radicals in CH_4/O_2 and C_2H_2/O_2 flames. *Proc. Combust. Inst,* **15**: 969.

Qin Z, Lissiansk WV, Yang H, Gardiner WC, Davis SG, Wang H. 2000. Combustion chemistry of propene: A case of detailed reaction mechanism optimization. *Proc. Combust. Inst.* **28**: 1663-1669.

Smith G, Golden D, Frenklach M, Moriarty N, Eiteneer B, Goldenberg M, Bowman C, Hanson R, Song S, Gardiner W, Lissianski V, Qin Z. 1999. GRI-Mech3.0, http://www.me.berkeley.edu/gri-mech/

Thomas SD, Bhargava A, Lindstedt PR, Westmoreland PR, Skevis G.1996. Propene oxidation chemistry in laminar premixed flames. *Bull. Soc. Chem. Belg.,* **105**: 501-512.

Varatharajan B, Williams FA. 2002. Ethylene ignition and detonation chemistry, part1: Detailed modelling and experiment comparison. *J. Propul. Power.,* **18**: 344-351.

Vardanyan I, Sachyan G, Nalbandyan, A. 1971. Kinetic and mechanism of formaldehyde oxidation. *Combust. Flame.,* **17**: 315.

Vardanyan I, Sachyan G, Philiposyan A, Nalbandyan A. 1974. Kinetic and Mechanism of Formaldehyde Oxidation – II. *Combust. Flame.,* **22**: 153.

Vovelle C, Foulatier R, Delbourgo R. 1971. Experimental device for probing gaseous samples out of a reaction and their subsequent injection into a chromatographic analyser. *Méthodes Phys. Anal.,* **7**(4): 353.

Warnatz J. 1984. Chemistry of high temperature combustion of alkanes up to octane. *Proc. Combust. Inst.,* **20**: 845-856.

Westbrook CK, Dryer FL, Shug KP. 1982. A comprehensive mechanism for the pyrolysis and oxidation of ethylene. *Proc. Combust. Inst.*, **19**: 153-166.

Westbrook CK, Thornton MM, Pitz WJ, Malte PC. 1988. Kinetic study of ethylene in a well-stirred reactor. *Proc. Combust. Inst.*, **22**: 863-871.

Won SJ, Ryu JC, Bae JH, Kim YD, Kang JG. 2000. Shock–tube study of the oxidation of acetaldehyde at high temperature. *Bull. Korean Chem. Soc.*, **21**(5): 487.

Yasunaga K, Kubo S, Hoshikawa H, Kamesawa T, Hidaka Y. 2007. Shock-tube and modeling study of acetaldehyde pyrolysis and oxidation. *Int. J. Chem. Kinet.*, **40**: 73.

Zervas E, Montagne X, Lahaye J. 1999. Influence of gasoline formulation on specific pollutants. *J. Air Waste Manage. Assoc.*, **49**: 1304-1314.

Zervas E, Montagne X, Lahaye J. 2001. C_1-C_5 organic acids emissions from a SI engine. Influence of fuel and air/fuel equivalence ratio. *Environ. Sci. Technol.*, **35**: 2746-2751.

Zervas E, Montagne X, Lahaye J. 2002. Emission of aldehydes and alcohols from SI engine. Influence of fuel and air/fuel equivalence ratio. *Environ. Sci. Technol.*, **36**: 2414-2421.

Zervas E. 2005. Formation of oxygenated compounds (Aldehydes, Alcohols, organic acids) from propane flames. *Envir. Engi. Sci.*, **22**: 651-659.